BNL C-A/AP/295

Optimized bunch patterns for d-Au in RHIC Run-8

W. Fischer and V. Ptitsyn

November 7, 2007

Abstract

With experience from previous runs we expect instabilities at transition to be the dominant intensity limiting effect for d-Au operation in Run-8. The beam intensity stability threshold is lowered by electron clouds, and the electron cloud density depends on the bunch pattern. We review bunch the pattern optimization in light of the operational experience in Run-7, and optimize the pattern for operation with two different species.

1 Introduction

Electron clouds in the PHOBOS experimental beam pipe have limited the RHIC luminosity in Run-4 and Run-5. Electron-impact desorption from electrons in the cloud led to an increased vacuum pressure, and subsequently to unacceptable background in the PHOBOS detector [1]. Under these circumstances, the average electron cloud density could be minimized, and the luminosity maximized, by distributing any given total intensity in as few bunches as possible, uniformly distributed along the circumference. This was found in simulations and supported by observations in experiments and operation [2–6].

Here we review the operational experience in Run-7, where at the end of the run the Au intensity was limited not by dynamic pressure rises, but by beam instabilities at transition. We then devise a strategy for maximizing the integrated luminosity by selecting the optimum bunch pattern for a given available bunch intensity for the Blue deuteron (d) beam, and the Yellow gold (Au) beams.

2 Operational experience with Au-Au in Run-7

Electron clouds limited the Au bunch intensity in Run-7. Initially, large dynamic pressure rises were observed at a few locations that could not be baked at high temperature. This could be remedied by 2 hours of scrubbing at injection with the highest available beam intensities, and further beam conditioning throughout the run [6].

At the end of the run, the Au intensity available at store was limited by beam instabilities at transition. These were previously identified as transverse single bunch instabilities [8], and two typical growth times were observed (15 ms and 120 ms). It is also known for some time that electron clouds at transition can lower the stability threshold [9]. A summary of single bunch instabilities due to electron clouds is Ref. [10].

Three measures were taken during the run to reduce the effect of the electron cloud on the beam stability at transition. First, the gap voltage at transition was lowered from 300 kV initially to 150 kV beginning at fill number 8799 (18 May 2007). With this bunches near transition are longer and the electron cloud density is lower. Second, the number of bunches was kept below the maximum of 111 in order to minimize transition losses. This yielded a visible improvement, making possible the acceleration of 103 bunches with up to 1.2×10^9 Au ions [11]. And third, the strength of the arc octupoles was increased compared to previous runs (see below).

Most of the physics stores had 103 bunches in each of the two rings. And almost all stores with 103 bunches had a bunch pattern shown in the lower part of Fig. 1. This pattern has 2 long gaps in addition to the abort gap, preserving the 3-fold symmetry that is necessary to obtain approximately the same number of collisions at both PHENIX and STAR.

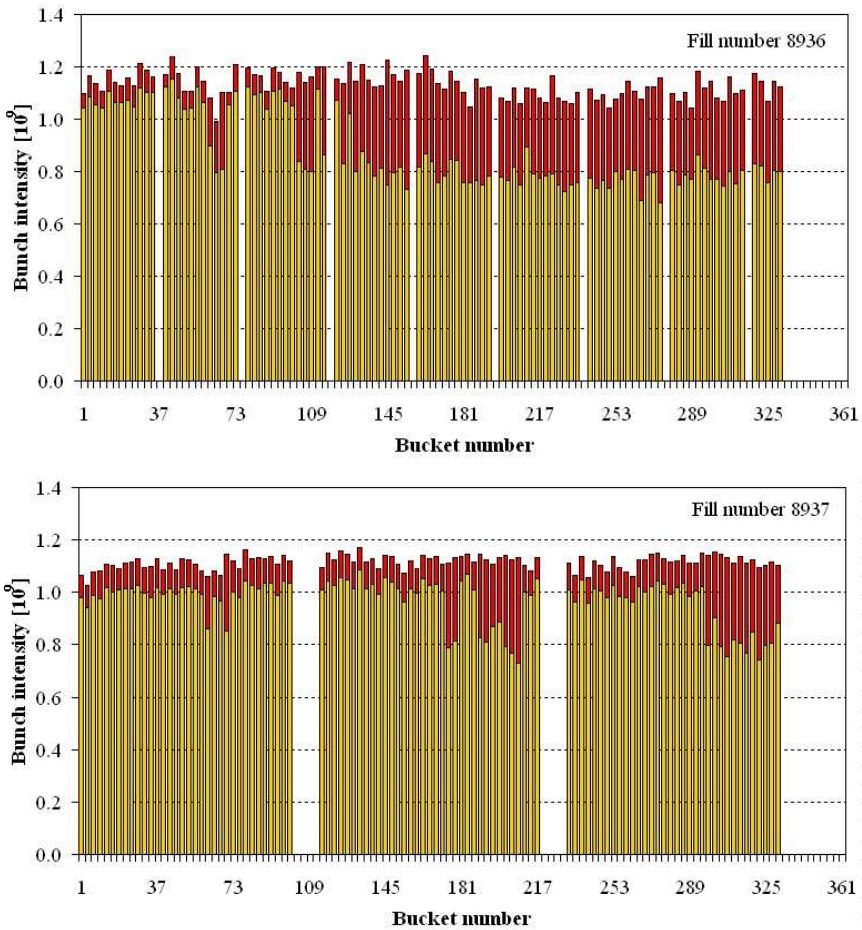

Figure 1: Yellow beam intensity before (red) and after (yellow) transition crossing for ramp 8936 with 8 short gaps (top), and ramp 8937 with 2 long gaps (bottom) in the bunch pattern. In addition to the gaps in the bunch pattern, there is the abort gap (8% of the circumference).

The used bunch pattern is, however, different from the pattern expected to minimize the average electron cloud density, which was found in previous simulations [3, 4]. This other pattern is shown in the upper part of Fig. 1. It has 8 small gaps, approximately uniformly distributed along the circumference, and the abort gap. This pattern too has a 3-fold symmetry. Although the amount of data is limited we now review the operational experience with the 2 patterns of 103 bunches.

Of all the 191 physics stores with 103 bunches, only the first 3 (fill numbers 8689, 8690, and 8693) had the pattern with 8 small gaps. In addition, ramp 8936 had this pattern (the ramp aborted). We compare the few cases with a pattern with 8 small gaps with the next 6 stores. The next 3 stores only had a different bunch pattern (and variations in the bunch intensity), for the following 3 stores the strength of the arc octupoles was increased from -5 m^{-3} to -6 m^{-3}.

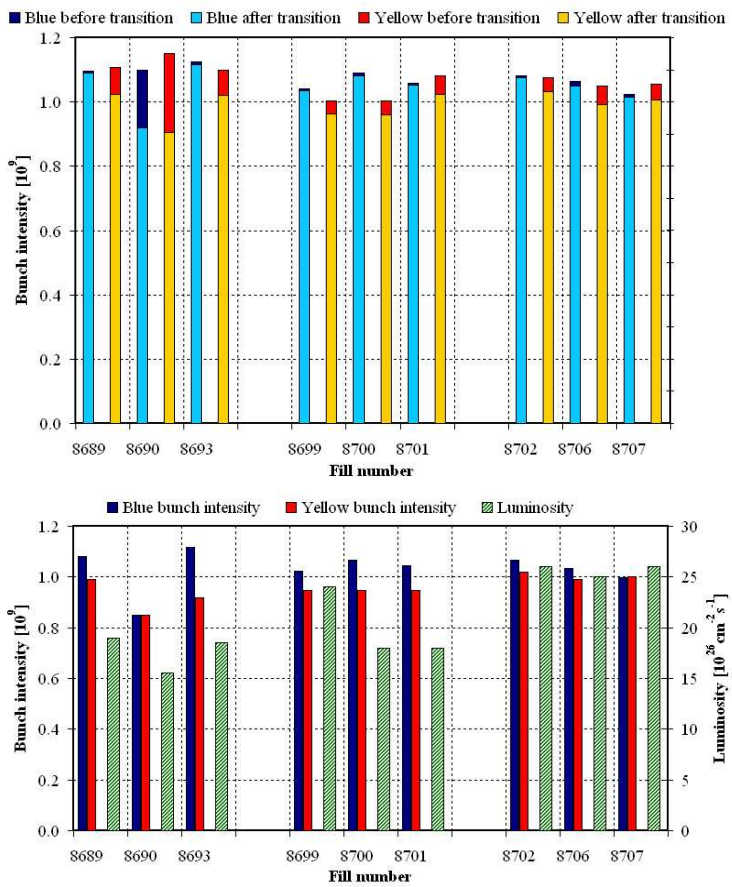

Figure 2: Comparison of different bunch patterns and octupole settings with 103 bunches. The first group of stores (8689, 8690, and 8693) has 8 small gaps, the second group (8699 to 8701) has 2 long gaps. The third group (8702 to 8707) also has 2 long gaps, and the arc octupole strength was increased from -5 m^{-3} to -6 m^{-3}. The top plot shows the Blue and Yellow average bunch intensities before and after transition crossing. The bottom plot shows the Blue and Yellow average bunch intensities, and the luminosity at the beginning of the store.

We first compare the 3 stores with 103 bunches and 8 small gaps (8689, 8690, and 8693) with the next 3 stores with 103 bunches that had 2 long gaps (8699, 8700, 8701). This is shown in Fig. 2. The upper part shows the Blue and Yellow average bunch intensity before and after transition. For the pattern with 8 short gaps the Yellow transition losses are generally larger, although the bunch intensities before transition are somewhat larger than for the ramps in the other group. The lower part of Fig. 2 shows the Blue and Yellow average bunch intensity, and the luminosity at the beginning of the stores. All 3 stores in the first group, and 2 out of 3 stores in the second group appear to have a significant number of bunches that experienced an instability at transition. After the arc octupole strength was increased from -5 m^{-3} to -6 m^{-3}, the situation is visibly improved, and all of the 3 stores that follow (8702, 8706, and 8707) have good luminosity. From this no clear preference for any of the 2 bunch patterns can be deduced.

We also note that the beam loss monitors aborted 30 ramps intended for physics [7]. With operation close to the instability threshold at transition, one should expect that the emittance of at least some bunches is increased regularly during transition crossing, making scraping during during beta squeeze more likely.

Table 1: List of input parameters for electron cloud simulations at transition.

parameter	unit	value
transverse beam offset	mm	0
bunches	...	103
rms beam radius	mm	1.5
pipe radius	mm	60
electrons generated/turn	10^7	2.4
electron generation radius	mm	1.15
full bunch length	m	1.2
bunch shape parameter n	...	3
bunch intensity	10^9 Au ions	1.0
longitudinal slices/turn	...	132000
macro-particles, initially	...	250
smoothing length d	mm	1.0
δ_{max}	...	1.95
E_{max}	eV	305
$E_{\text{secondary}}$	eV	8.925
P_0	...	0.5
E_{reflect}	eV	60
s	...	1.813
$P_{\text{rediffuse}}$	...	0.5
α_δ	...	0.5
α_θ	...	1.0
P_∞	...	0.1

We now compare the two patterns in a simulation with CSEC [12], where we use the parameters shown in Tab. 1. These are for conditions in the field free warm straight sections, with stainless steel, at transition. The result is shown in Fig. 3. The average

electron cloud density of the two patterns is not very different, but the range of electron cloud density within one turn is quite different. The pattern with 2 long gaps has a much wider range, dipping lower after each gap and rising higher before the next gap. If the onset of a beam instability requires a minimum electron cloud density, the simulation result could explain why the pattern with 2 gaps leads to fewer unstable bunches. For example, if for the situation depicted in Fig. 3 0.25 nC/m were required for bunches to become unstable, almost all bunches in the pattern with 8 short gaps would be unstable, but fewer bunches in the pattern with 2 long gaps.

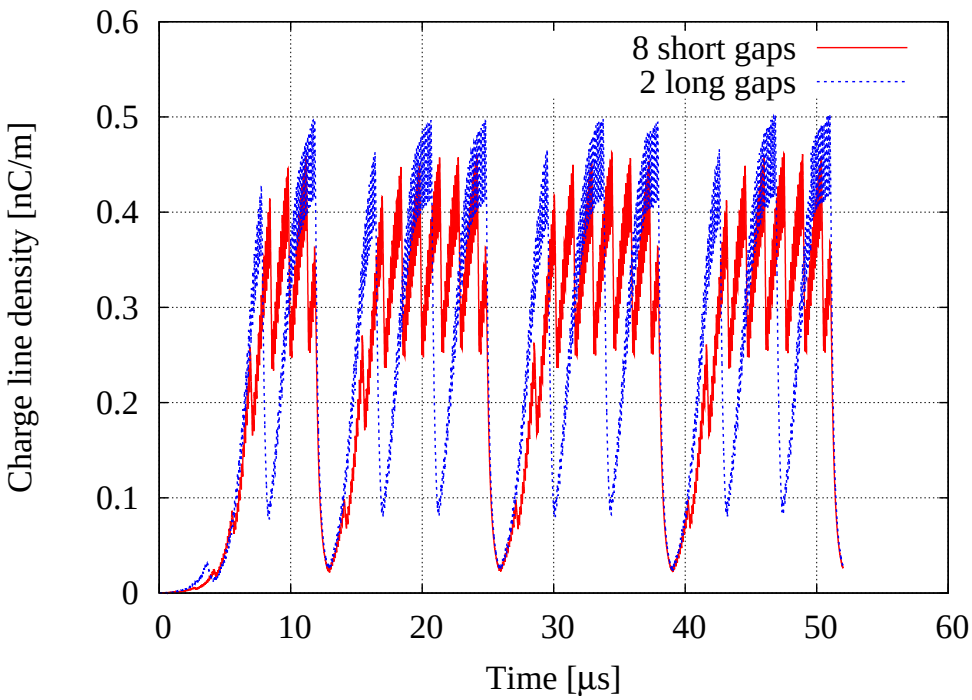

Figure 3: Simulated electron cloud build-up over 4 turns with 103 bunches and different bunch patterns. Like during Run-7, patterns with 8 short and 2 long gaps are shown. Simulation parameters are listed in Tab. 1.

The effect of the transition instabilities on the luminosity is shown in Fig. 4, where the initial luminosity is depicted as a function of the Blue total, Yellow total, and Blue+Yellow total intensity for all physics stores of Run-7. Most of these stores had the bunch pattern with 103 bunches and 2 long gaps. For increasing intensities the initial luminosity increase at first, but decreases beyond a certain intensity value. It is difficult to establish the intensity above which no further luminosity increase can be expected during a run, since the initial luminosities have a wide range for any given intensity.

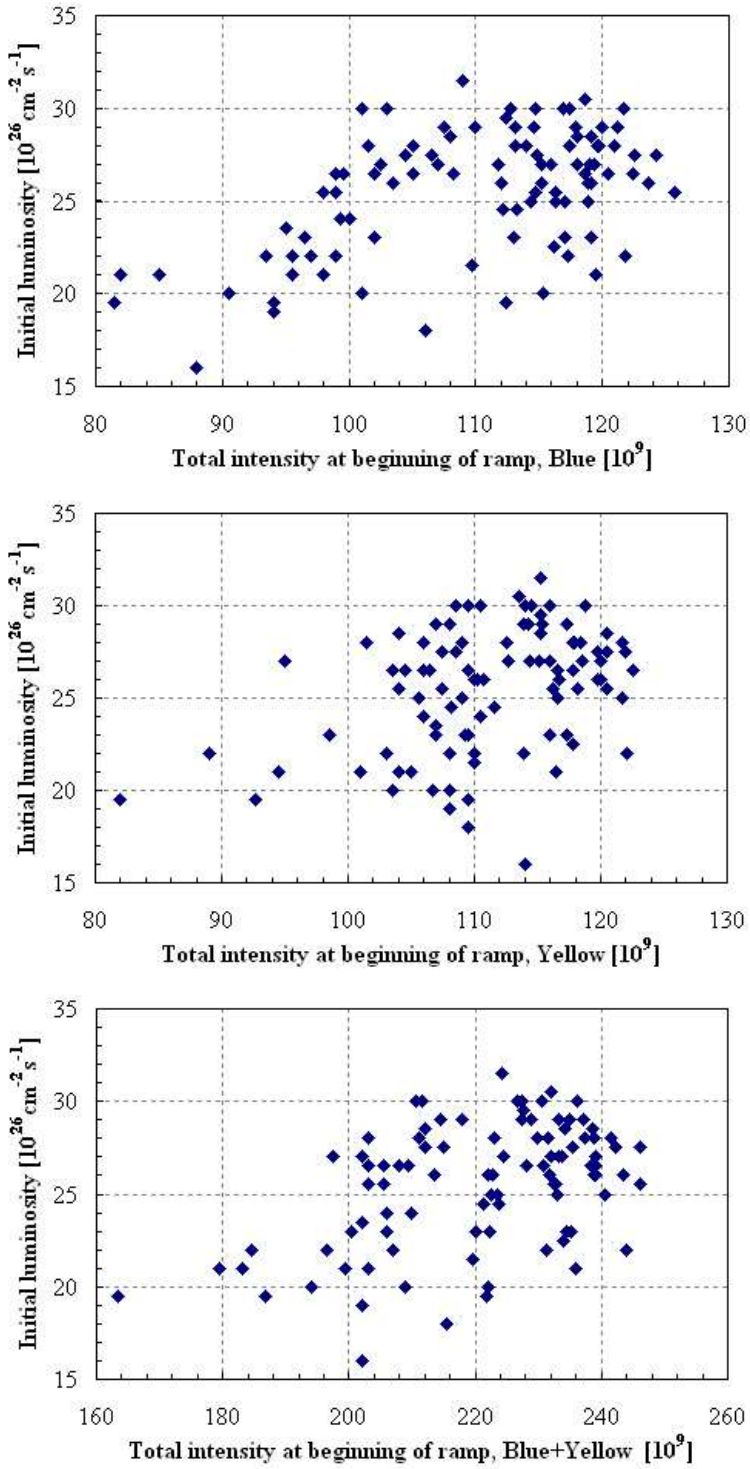

Figure 4: Initial luminosity as a function of the Blue beam total intensity at the beginning of the ramp (top), Yellow beam total intensity (middle) and, the sum of Blue and Yellow intensities. Shown are all 229 physics store of Run-7, of which 191 had a pattern with 103 bunches and 2 long gaps.

Table 2: Expected maxima for number of bunches and bunch intensities for Run-8. These maxima may not be attainable simultaneously.

parameter	unit	d (Blue)	Au (Yellow)
number of bunches N_{max0}	...	111	
bunch intensity $N_{B,Y,max0}$	10^9	120	1.1
charges per bunch N_c	$10^{11}e^+$	1.2	0.9

3 Bunch patterns for d-Au in Run-8

The time dependent luminosity $\mathcal{L}(t)$ is given by

$$\mathcal{L}(t) = \frac{3F}{\pi}(\beta\gamma)\frac{f_{rev}N}{\beta^*}\frac{N_B(t)N_Y(t)}{\epsilon_B(t)+\epsilon_Y(t)} \tag{1}$$

where F is a factor that accounts for luminosity losses due to a crossing angle and the hourglass effect, $(\beta\gamma)$ are the relativistic factors, f_{rev} is the revolution frequency, N is the number of bunch collisions per turn, and β^* the lattice function at the interaction point (IP). N_B and N_Y denote the Blue and Yellow bunch intensities, respectively, and ϵ_B and ϵ_Y the Blue and Yellow normalized emittances,

$$\epsilon_{B/Y} = (\beta\gamma)\frac{6\sigma^2_{B/Y}}{\beta}, \tag{2}$$

with β the lattice function here. We have assumed round beams for both the Blue and Yellow beam,

$$\epsilon_{x,B} = \epsilon_{y,B} = \epsilon_B \qquad \text{and} \qquad \epsilon_{x,Y} = \epsilon_{y,Y} = \epsilon_Y \tag{3}$$

but not necessarily the same emittance of the Blue d beam, and the Yellow Au beam. For collisions without a crossing angle the hourglass reduction factor is [13]

$$F = \int_{-\infty}^{\infty}\frac{dt}{\sqrt{\pi}}\frac{\exp(-t^2)}{\sqrt{(1+t^2/t_x^2)(1+t^2/t_y^2)}} \tag{4}$$

with

$$t_x^2 = \frac{2(\sigma^{*2}_{x,B}+\sigma^{*2}_{x,Y})}{(\sigma^{*2}_{z,B}+\sigma^{*2}_{z,Y})(\sigma^{*2}_{x,B}/\beta^{*2}_{x,B}+\sigma^{*2}_{x,Y}/\beta^{*2}_{x,Y})} \tag{5}$$

and a similar expression for t_y. In our situation we have $\beta^* = 1$ m and $F = 0.96$ at the beginning of a store.

We now need to find the values for (N, N_B, N_Y) and the bunch pattern that maximize the luminosity $\mathcal{L}$. Tab. 2 shows the expected maxima for the number of bunches, and the d and Au bunch intensities. For the optimization we require that no bunches become unstable at transition. It is possible that a slightly higher luminosity can be obtained when a limited number of bunches become unstable. The optimization for the luminosity $\mathcal{L} \propto NN_BN_Y$ can be done with the following steps:

1. We find the bunch pattern that is best to avoid instabilities at transition.

2. We assume that $N_B = N_{B,max}$ and $N_Y = N_{Y,max}$ has been reached with small N. We then increase N, using the best bunch patterns, until one of the beams encounters the transition instability. This is more likely in the Blue ring since more charges per bunch will be available for the Blue beam. That yields the luminosity $\mathcal{L}_1$.

3. We now increase N and decrease N_B with $NN_B = \text{const}$ until the transition instability in Yellow is encountered, or $N = N_{max}$. With no reduction in the luminosity we have reduced the maximum electron cloud density in Blue.

4. We can now increase the Blue bunch intensity N_B again until the transition instability is encountered or its maximum value reached.

While the above steps lead to the maximum luminosity we still need to find the optimum bunch patterns for a given total intensity. In addition to the simulation presented in the previous section, Fig. 5 shows electron cloud built-up simulations for a given total intensity and different number of bunches, for patterns with 2 large, and many small gaps.

It is noteworthy to compare for all cases the charge line density averaged over one turn (turn 4 in the simulation), the maximum charge line density, and the minimum charge line density in each turn after the electron cloud build-up is complete. This is shown in Fig. 6. For the range of bunch numbers tested the average electron cloud density does not change much, and is not very different for the two bunch patterns. For smaller bunch numbers a difference between the bunch number becomes visible. This is consistent with earlier simulations for 68 bunches [2, 3].

While the average electron cloud density per turn is about the same for all cases tested, the range and the maximum the density is much larger for the patterns with 2 large gaps. To suppress the instabilities in all bunches the instability threshold must be above the maximum. For any given total intensity, patterns with many small gaps are therefore favorable to suppress instabilities in all bunches. This conclusion could also be tested in operation in Run-8.

4 Summary

Based on the analysis of Run-7 data, and electron cloud build-up simulations one can expect that to suppress transition instabilities in all bunches, patterns with many small gaps, distributed evenly over the circumference are best. These patterns minimize the maximum electron cloud density. With this the bunch intensities N_B, N_Y and the number of bunches N can be chosen according to the prescription in Sec. 3 in order to maximize the luminosity $\mathcal{L}$.

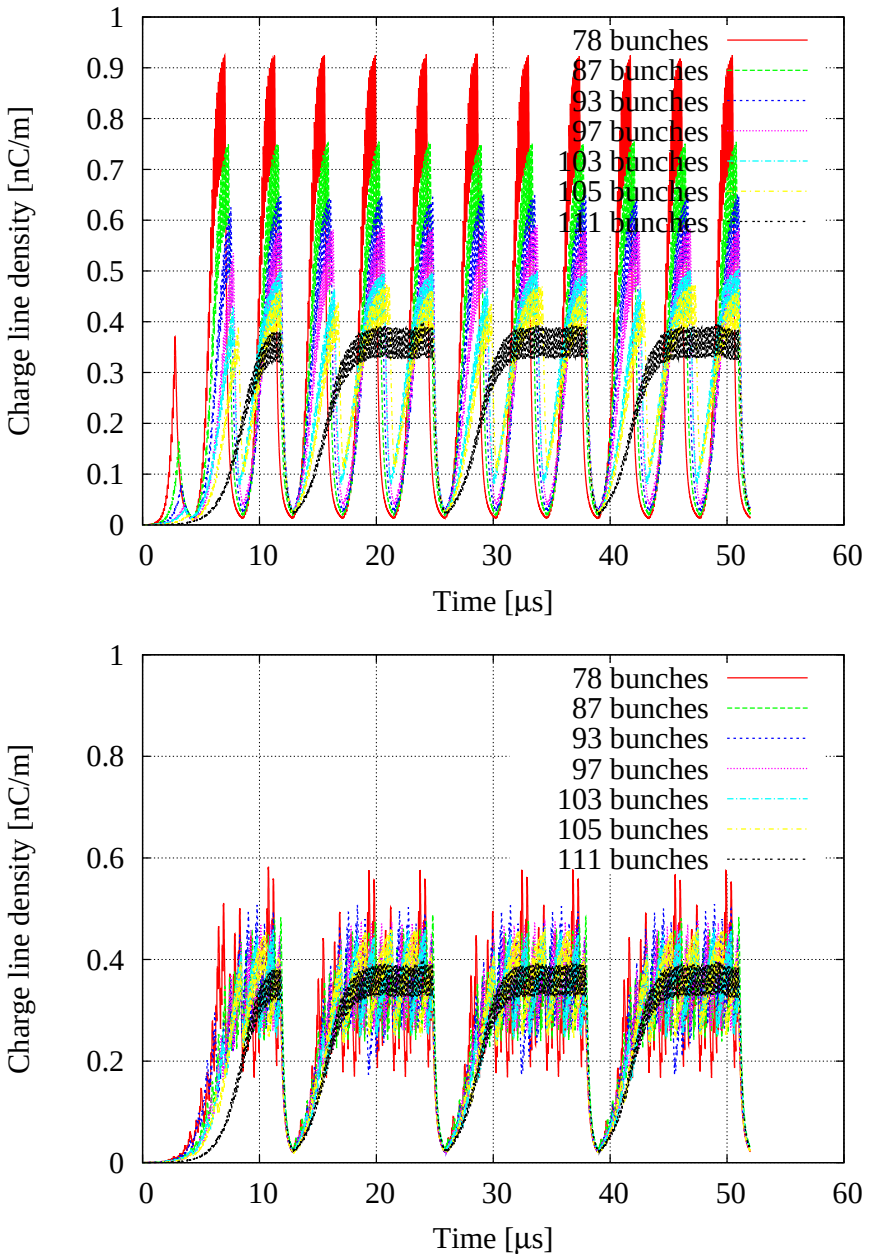

Figure 5: Simulated electron cloud densities over 4 turns for the same total intensity but different number of bunches. The upper plot shows bunch patterns with 2 long gaps, the lower plot shows patterns with many small gaps, distributed approximately uniformly around the circumference.

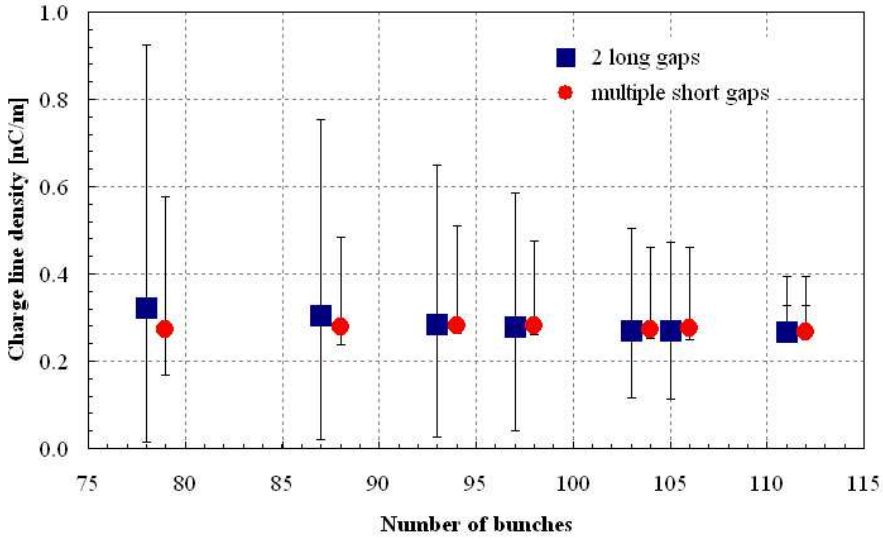

Figure 6: Electron cloud density averaged over one turn, maximum electron cloud density (upper bar), and minimum electron cloud density per turn after the cloud build-up has finished (lower bar) for all bunch cases shown in Fig. 5. The number of bunches for the cases with multiple short gaps are increase by one for better readability.

5 Acknowledgments

The authors are thankful to M. Bai, M. Blaskiewicz, K. Brown, A. Drees, K. Gardner, U. Iriso, M. Mapes, T. Roser, and S.Y. Zhang for help, comments and discussions.

References

[1] G. Rumolo and W. Fischer, "Observations on background in PHOBOS and related electron cloud simulations", BNL C-A/AP/146 (2004).

[2] W. Fischer and U. Iriso, "Bunch patterns and pressure rise in RHIC", proceedings of the 2004 European Particle Accelerator Conference, Lucerne (2004).

[3] W. Fischer and U. Iriso-Ariz, "Bunch patterns and pressure rise in RHIC", BNL C-A/AP/118 (2003).

[4] W. Fischer, L. Ahrens, J. Alessi, M. Bai, D. Barton, J. Beebe-Wang, M. Blaskiewicz, J.M. Brennan, D. Bruno, J. Butler, R. Calaga, P. Cameron, R. Connolly, J. Delong, T. D'Ottavio, A. Drees, W. Fu, G. Ganetis, W. Glenn, T. Hayes, P. He, H. Huang, H.C. Hseuh, P. Ingrassia, U. Iriso, R. Lee, Y. Luo, G. Marr, W.W. MacKay, A. Marusic, R. Michnoff, C. Montag, J. Morris, T. Nicoletti, B. Oerter, S. Peggs, A. Pendzick, C. Pearson, F. Pilat, V. Ptitsyn, T. Roser, J. Sandberg, T. Satogata, C. Schultheiss, A. Sidi-Yekhlef, L. Smart, S. Tepikian, R. Tomas, N. Tsoupas, D. Trbojevic, J.

Tuozzolo, K. Vetter, K. Yip, A. Zaltsman, A. Zhang, S.Y. Zhang, J. van Zeijts, and the RHIC Operations Team, "Luminosity increases in gold-gold operation in RHIC", proceedings of the 2004 European Particle Accelerator Conference, Lucerne (2004).

[5] F. Pilat, L. Ahrens, M. Bai, D.S. Barton, J. Beebe-Wang, M. Blaskiewicz, J.M. Brennan, D. Bruno, P. Cameron, R. Connolly, J. DeLong, T. D'Otavio, A. Drees, W. Fischer, G. Ganetis, C. Gardner, J. Glenn, P. Harvey, T. Hayes, H.-C. Hseuh, H. Huang, P. Ingrassia, U. Iriso, R. Lee, V.N. Litvinenko, Y. Luo, W.W. MacKay, G. Marr, A. Marusic, R. Michnoff, C. Montag, J. Morris, A. Nicoletti, B. Oerter, V. Ptitsyn, T. Roser, T. Russo, J. Sandberg, T. Satogata, C. Schultheiss, S. Tepikian, R. Tomas, D. Trbojevic, N. Tsoupas, J. Tuozzolo, K. Vetter, A. Zaltsman, K. Zeno, S.Y. Zhang, W. Zhang, "Operations and performance of RHIC as a Cu-Cu collider", proceedings of the 2005 Particle Accelerator Conference, Knoxville, Tennessee (2005).

[6] W. Fischer, M. Blaskiewicz, M. Brennan, H. Huang, H.-C. Hseuh, V. Ptitsyn, T. Roser, P. Thieberger, J. Wei, and S.Y. Zhang, "Electron cloud observations and cures in RHIC", proceedings of the ECLOUD'07 workshop, Daegu, Korea (2007). [submitted to Phys. Rev. ST Accel. Beams]

[7] M. Bai, private communication (2007).

[8] M. Blaskiewicz, J.M. Brennan, P. Cameron, C. Dawson, C. Degan, K. Drees, W. Fischer, E. Koropsak, R, Michnoff, C. Montag, T. Roser, T. Satogata, and N. Catalan-Lasheras, "Transverse instabilities in RHIC", proceeding of the 2003 Particle Accelerator Conference, Portland, OR (2003).

[9] J. Wei et al., "Electron clouds and single-bunch instabilities in the Relativistic Heavy Ion Collider", proceedings of the 39th ICFA Advanced Beam Dynamics Workshop on High Intensity High Brightness Hadron Beams HB2006, Tsukuba, Japan (2006).

[10] F. Zimmermann, "Review of single bunch instabilities driven by an electron clouds" Phys. Rev. ST - Accel. Beams **7**, 124801 (2004).

[11] V. Ptitsyn, RHIC e-log entry 18 May 2007, 14:34.

[12] M. Blaskiewicz and U. Iriso, "How to use CSEC", BNL C-A/AP/260 (2006).

[13] M.a. Furman and M.S. Zisman, "Luminosity", in "Handbook of accelerator physics and engineering", 3rd printing, World Scientific (2006).